ELSEVIER

Microstructural Based Modelling of the Elastic Modulus of Fiber Reinforced Cement Composites

Albert Ngollè and Jean Péra
Unité de Recherche Génie Civil-Matériaux, Institut National des Sciences Appliquées de Lyon, Villeurbanne, France

In this work, a new analytical model for predicting the elastic modulus of discontinuous fiber reinforced cement composites in uniaxial tension is presented. The proposed elastic modulus model depends on the macroscopic and microstructural parameters (interfacial bond modulus, matrix porosity, and so forth) of the composite. The microstructural scale is the fiber. The composite is considered to be a set of many fiber-matrix cells. The shear-lag concept is used to determine the forces and stress fields in the unit cell. The linkage between the microstructural and the macroscopic properties (homogenization) is made through an averaging process based on continuum mechanics, probabilistic considerations, and tensorial transformations. The model is applicable to all fiber orientations, probabilistic or deterministic. The particularities are that the model is triphasic and integrates the probabilistic density function of fiber orientation as a variable. Good agreement is observed between the model predictions and the limited experimental data available. The model is applicable to other discontinuous fiber reinforced quasibrittle matrix composites. ADVANCED CEMENT BASED MATERIALS 1997, 6, 130–137. © *1997 Elsevier Science Ltd.*

KEY WORDS: Composite, Elastic modulus, Fiber cement composite, Homogenization, Probabilistic orientation, Shear-lag concept, Quasibrittle matrix composite, Unit cell

The elastic modulus is an essential material characteristic of fiber reinforced cement composites (FRC). Reliable models are needed for design and optimization of FRC. For this purpose, many models have been developed. Some models are based on the rule of mixtures, such as those of Krenchel [1], Nielsen and Chen [2], Allen [3], Shah and Rangan [4], Pakoriprapha et al. [5], and Naaman et al. [6]. These models have the characteristic to be biphasic; that is, a perfect bond is considered to be between the fiber and the matrix. Baalbaki et al. [7] showed that biphasic models do not properly describe the behavior of composites. Thus, it is necessary to consider the interfacial layer as a third phase when modelling the behavior of FRC. Fortunately, many studies such as Bentur et al. [8] have addressed the characterization of interfacial properties of FRC. Alwan and Naaman [9] have developed a triphasic model for the elastic modulus of random short fiber composites. In their approach, the interfacial layer surrounding the fiber is considered to be a third phase with zero volume and is modelled as an imperfect bond with its own mechanical properties. In addition to the triphasic characteristic, there is also a need for clarification of the probabilistic characteristic of the fibers' orientation in the composite.

For this reason, our goal was to make the analytical model presented in this study triphasic and to integrate the probabilistic density function of fiber orientation as a variable. Thus, it is applicable to all cases of fiber orientation in the composite, whether probabilistic or deterministic.

In this approach (as in Alwan and Naaman's approach [9]), the microstructural element is the fiber-matrix cell, and the shear-lag concept is used to determine the forces and stress fields in the cell. The linkage between the microstructural and macroscopic properties is achieved through an averaging process based on continuum mechanics, probabilistic considerations, and tensorial transformations. The model validation is made with the help of experimental data from tests conducted by the authors and tests available in the literature.

Equilibrium of a Unit Cell in Tension

The stress fields in the fiber-matrix cell are determined by using the shear-lag concept [9,10] (Figure 1). The unit cell has the same fiber volume ratio as the composite. The derivation of the differential equation for the axial

Address correspondence to: Albert Ngollè, Unité de Recherche Génie Civil-Matériaux, Institut National des Sciences Appliquées de Lyon, 20, Avenue Albert Einstein, Bâtiment 407, 69621 Villeurbanne, France.
Received March 21, 1997; Accepted August 8, 1997

ISSN 1065-7355/97/$17.00
PII S1065-7355(97)00037-0

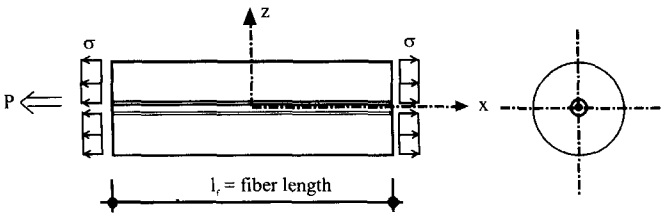

FIGURE 1. Unit cell in uniaxial tension.

force in the fiber is the same as that given in ref 9, which leads to

$$\frac{d^2f(x)}{dx^2} - ck\alpha f(x) + \frac{ckP}{E_m a_m} = 0 \tag{1}$$

where E_m and E_f are the elastic moduli of the matrix and the fiber, respectively; a_c, a_m, and a_f are the cross sectional areas of the unit cell, the matrix, and the fiber, respectively; c is the fiber circumference; k is the interfacial shear bond modulus; $f(x)$ is the axial force in the fiber; P is the result of the forces in the cross section of the unit cell, and

$$\alpha = \frac{1}{E_f a_f} + \frac{1}{E_m a_m}. \tag{2}$$

The general solution of eq 1 can be written as:

$$f(x) = A\ cosh(\beta x) + B\ sinh(\beta x) + F \tag{3}$$

where A and B are constants;

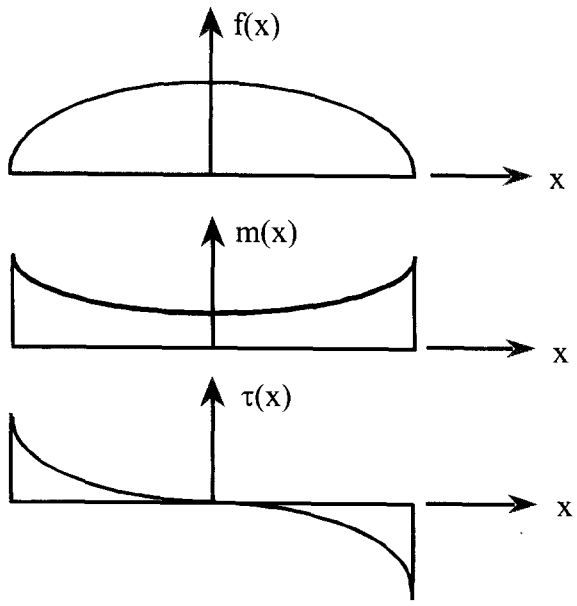

FIGURE 2. Qualitative representation of forces and stress in the cell.

$$\beta = \sqrt{ck\alpha} \text{ and } F = \frac{P}{\alpha E_m a_m}. \tag{4}$$

The axial force in the fiber is assumed to be equal to zero at its extremities (because of the small cross sectional area of the fiber and the negligible perpendicular bond). Thus, the boundary conditions of eq 1 can be written as:

$$f(x = -L) = f(x = L) = 0. \tag{5}$$

The expressions of the forces in the fiber [$f(x)$], in the matrix [$m(x)$], and the interfacial stress [$\tau(x)$] can then be derived, knowing that

$$m(x) = P - f(x) \tag{6}$$

and

$$\tau(x) = \frac{1}{c}\frac{df(x)}{dx} \tag{7}$$

$$f(x) = F\left(1 - \frac{cosh(\beta x)}{cosh(\beta L)}\right) \tag{8}$$

$$m(x) = \alpha E_m a_m F - F\left(1 - \frac{cosh(\beta x)}{cosh(\beta L)}\right) \tag{9}$$

$$\tau(x) = -\frac{F\beta}{c}\left(\frac{sinh(\beta x)}{cosh(\beta L)}\right). \tag{10}$$

The relationships of these equations are illustrated in Figure 2.

Consideration of the Increase of Matrix Porosity Due to the Presence of Fibers

The presence of fibers in the composite increases its matrix porosity [6,12]. The matrix porosity in presence of fibers is given by the relation of Allen [3]:

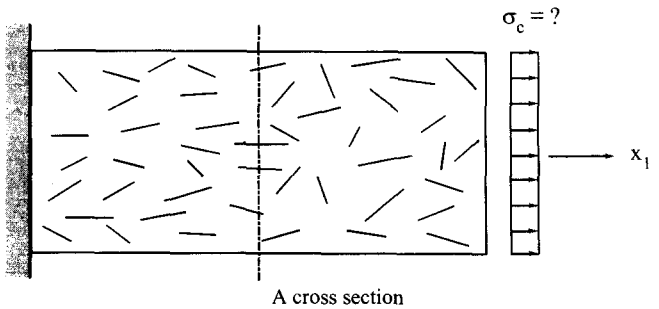

FIGURE 3. Composite under uniaxial tension.

Adv Cem Bas Mat
1997;6:130–137

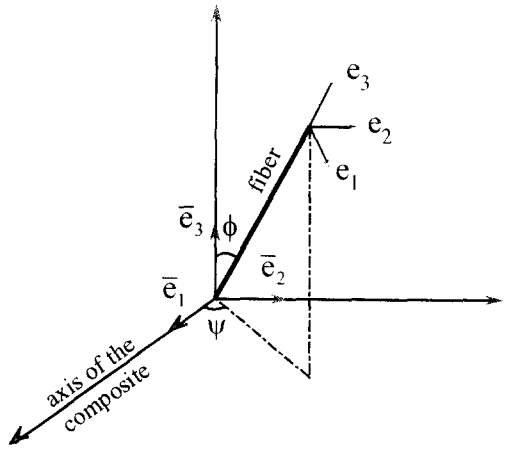

FIGURE 4. Global and local coordinates.

$$\xi = \xi_0 + rV_f \tag{11}$$

where ξ_0 is the matrix porosity without fibers and r is a coefficient depending on the matrix and the fiber properties (e.g., type, surface, geometry). The formula derived by Kendall [11] can be used to describe the link between the modulus E_m with ξ porosity and the matrix modulus E_{m00} with zero porosity:

$$E_m = E_{m00}(1 - \xi)^3. \tag{12}$$

The relationship between the matrix modulus with ξ porosity E_m and the one with ξ_0 porosity E_{m0} can be written as [12]:

$$E_m = E_{m0}\left(\frac{1 - \xi}{1 - \xi_0}\right)^3. \tag{13}$$

E_m as defined in eq 13 is used in this article.

The Elastic Modulus of the Composite

In general, the elasticity tensor is a fourth order symmetric tensor of components E_{ijkl}. It is stated that E_c is the component of the elasticity tensor in the direction of the composite axis (direction of traction). In what follows E_c is modelled for any fiber orientation in the composite; that is, E_c depends on the probability density function for fiber orientation $g(\phi,\psi)$.

Assuming the composite is under uniaxial tension, the cross section appears as in Figure 3. The matrix stress σ_m in the composite cross section is assumed to be constant. The axial force in the fibers in the composite cross section can be determined as a function of σ_m. Thus, considering the number of fibers crossing the section, and using probabilistic averages for fibers, the average stress σ_c (and strain ε_c) of the composite cross section can be determined as a function of σ_m. The composite elastic modulus can then be derived from the relation $E_c = \sigma_c/\varepsilon_c$.

The orientation angles of a fiber crossing the composite section are ϕ and ψ (Figure 4). The matrix stress tensor expressed in global coordinates basis $(\bar{e}_1, \bar{e}_2, \bar{e}_3)$ is

$$[\bar{\sigma}_{ij}] = \begin{bmatrix} \sigma_m & 0 & 0 \\ 0 & 0 & 0 \\ 0 & 0 & 0 \end{bmatrix}. \tag{14}$$

The expression of the same tensor in the local coordinates basis, fiber basis (e_1, e_2, e_3), is

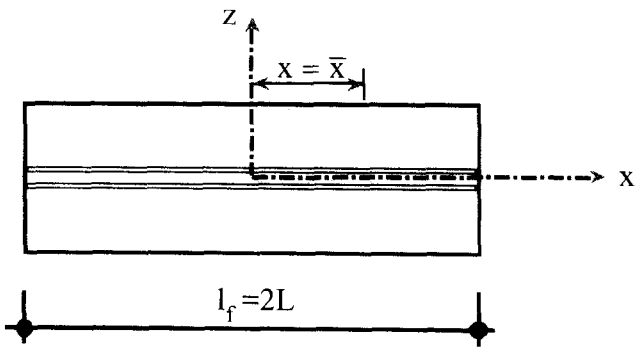

FIGURE 5. Fiber-matrix cell; intersection with composite cross section.

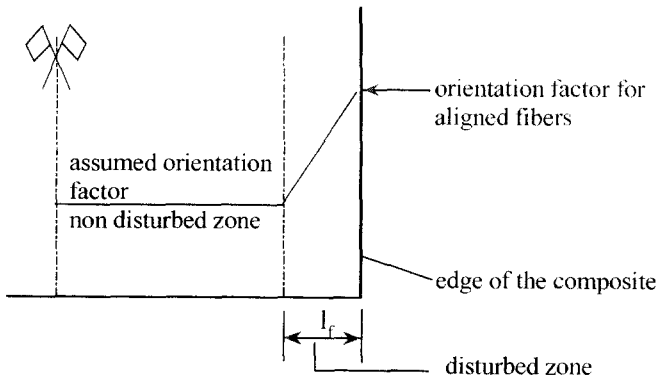

FIGURE 6. A way to approximate the effect due to the surface of a mold.

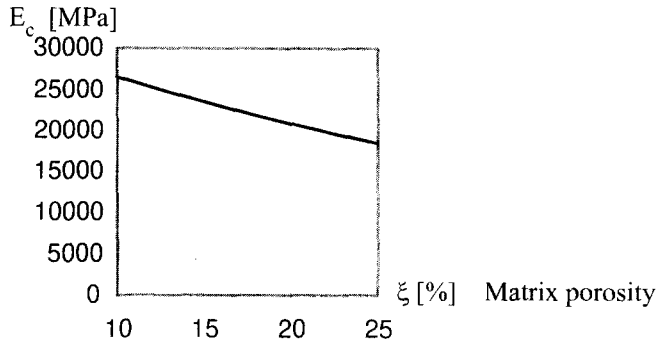

FIGURE 7. Influence of the matrix porosity on the composite elastic modulus.

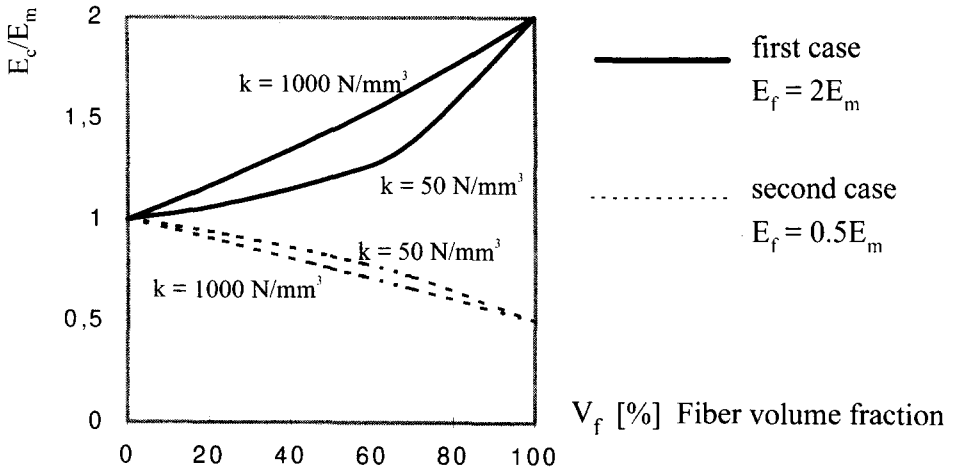

FIGURE 8. The effect of the bond modulus on the composite elastic modulus.

$$[\sigma_{ij}] = \sigma_m \begin{bmatrix} cos^2\,\phi\, cos^2\,\psi & -cos\,\psi\, cos\,\phi\, sin\,\psi & cos^2\,\psi\, cos\,\phi\, sin\,\phi \\ -cos\,\psi\, cos\,\phi\, sin\,\psi & sin^2\,\psi & -cos\,\psi\, sin\,\phi\, sin\,\psi \\ cos^2\,\psi\, cos\,\phi\, sin\,\phi & -cos\,\psi\, sin\,\phi\, sin\,\psi & sin^2\,\phi\, cos^2\,\psi \end{bmatrix}. \tag{15}$$

A unit fiber-matrix cell formed around the fiber is considered. Assuming this fiber crosses the composite section at $x = \bar{x}$ in the local coordinates, the result is as shown in Figure 5.

The matrix stress at point $x = \bar{x}$ is equal to the component of the $[\sigma_{ij}]$ tensor in the direction of the fiber axis:

$$\sigma_{33} = \sigma_m\, sin^2\,\phi\, cos^2\,\phi. \tag{16}$$

The force in the matrix at the intersection point $x = \bar{x}$ is thus

$$m(x = \bar{x}) = \sigma_{33} a_m. \tag{17}$$

(The effect of the other components of the $[\sigma_{ij}]$ tensor are neglected.)

Considering eq 8 and 9, the force in the fiber at the intersection point $x = \bar{x}$ can be determinated as follows:

$$f(\bar{x}) = \sigma_{33} a_m \frac{cosh(\beta L) - cosh(\beta \bar{x})}{\frac{E_m a_m}{E_f a_f} cosh(\beta L) + cosh(\beta \bar{x})} \tag{18}$$

that is,

$$f(\bar{x}) = \sigma_{33} a_m \lambda(\bar{x}) \tag{19}$$

with

$$\lambda(\bar{x}) = \frac{cosh(\beta L) - cosh(\beta \bar{x})}{\frac{E_m a_m}{E_f a_f} cosh(\beta L) + cosh(\beta \bar{x})}. \tag{20}$$

Using symmetrical considerations, the average value of $f(\bar{x})$ is determined by:

TABLE 1. Comparison of test results with model predictions

		E_c [Mpa]			
		Experimentation			
	V_f [%]	Number of Tests	Average	Model	Discrepancy
Polypropylene-FRC	2%	4	18643 ± 174	18970	1.8%
	3%	4	18595 ± 249	18955	1.9%
	4%	2	18329 ± 382	18939	3.3%
Metallic-FRC	3%	3	19784 ± 468	19247	2.7%
Glass-FRC	4%	3	19712 ± 926	19334	2.0%

Adv Cem Bas Mat
1997;6:130–137

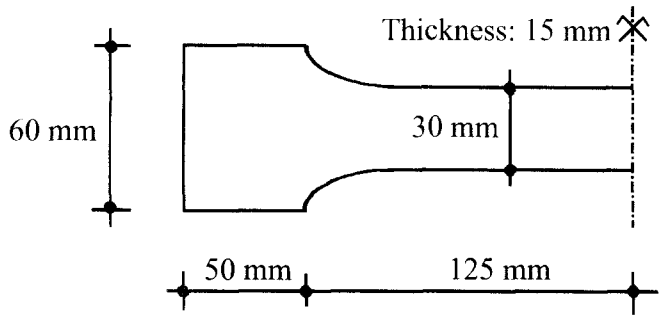

FIGURE 9. Specimen geometry.

$$\langle f(\bar{x})\rangle = \frac{1}{L}\int_0^L f(\bar{x})d\bar{x} = \sigma_{33}a_m\frac{1}{L}\int_0^L \lambda(\bar{x})d\bar{x}$$

$$= \sigma_{33}a_m\langle\lambda(\bar{x})\rangle. \tag{21}$$

The evaluation of $\langle\lambda(\bar{x})\rangle$ leads to:

$$\sigma_m A_m + \langle N_f\rangle\langle f_f\rangle = \sigma_c A_c. \tag{25}$$

$$\langle N_f\rangle = \frac{A_c}{a_f} V_f\langle sin\ \phi\ cos\ \psi\rangle \tag{26}$$

is the number of fibers in the composite cross section (from geometrical and probabilistic considerations [13]); V_f is the fiber volume fraction in the composite; A_c and a_m are the cross sectional areas of the composite and the matrix, respectively. σ_c can in this way be expressed by:

$$\sigma_c = \sigma_m(1 - V_f)(1 + \langle\lambda(\bar{x})\rangle\eta_1^2\eta_2). \tag{27}$$

The corresponding average composite strain can be derived by using the averaging relation between the macroscopic stress tensor ε_{ij} and the microscopic one $\varepsilon_{ij}^{\varepsilon}$ in a volume ΔV.

$$\varepsilon_{ij} = \frac{1}{\Delta V}\int_{\Delta V}\varepsilon_{ij}^{\varepsilon}dV. \tag{28}$$

$$\langle\lambda(\bar{x})\rangle = \begin{cases} -1 + \dfrac{q_1 + q_2}{\beta L q_3}\left(ln\left|\dfrac{e^{\beta L} + q_2 - q_3}{e^{\beta L} + q_2 + q_3}\right| - ln\left|\dfrac{1 + q_2 - q_3}{1 + q_2 + q_3}\right|\right) & \text{for } q_2 > 1 \\ -1 + \dfrac{q_1 + q_2}{\beta L}\left(\dfrac{2}{q_2 + 1} - \dfrac{2}{e^{\beta L} + q_2}\right) & \text{for } q_2 = 1 \\ -1 + 2\dfrac{q_1 + q_2}{\beta L q_4}\left(arctan\left[\dfrac{e^{\beta L} + q_2}{q_4}\right] - arctan\left[\dfrac{q_2 + 1}{q_4}\right]\right) & \text{for } q_2 < 1 \end{cases} \tag{22}$$

with $q_1 = cosh(\beta L)$; $q_2 = E_m a_m / E_f a_f\, q_1$; $q_3 = \sqrt{q_2^2 - 1}$; $q_4 = \sqrt{1 - q_2^2}$.

The component of $\langle f(\bar{x})\rangle$ in the direction of the axis of the composite $\bar{e}_1$ is

$$\langle f(\bar{x})\rangle sin\ \phi\ cos\ \psi = \sigma_{33}a_m\langle\lambda(\bar{x})\rangle sin\ \phi\ cos\ \psi$$

$$= \sigma_m\, sin^2\ \phi\ cos^2\ \psi a_m\langle\lambda(\bar{x})\rangle$$

$$\times\ sin\ \phi\ cos\ \psi. \tag{23}$$

The generalization of this expression for all fibers in the cross section is called $\langle f_f\rangle$ and occurs through the application of the mathematical expectation operator $\langle\cdot\rangle$ over the orientation angles.

$$\langle f_f\rangle = \sigma_{33}a_m\langle\lambda(\bar{x})\rangle\langle sin^2\ \phi\ cos^2\ \psi\rangle\langle sin\ \phi\ cos\ \psi\rangle$$

$$= \sigma_{33}a_m\langle\lambda(\bar{x})\rangle\eta_2\eta_1 \tag{24}$$

with $\eta_2 = \langle sin^2\ \phi\ cos^2\ \psi\rangle$ and $\eta_1 = \langle sin\ \phi\ cos\ \psi\rangle$.

The composite average stress σ_c can be determinated with the help of the equilibrium of forces in the cross section.

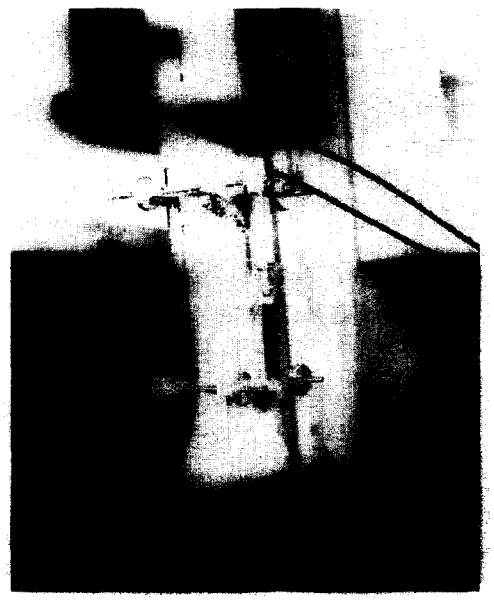

FIGURE 10. Test set-up for uniaxial tension.

TABLE 2. Comparison of model predictions with test results of Alwan and ROM's predictions

	V_f [%]	16	16.3	17	24	26
E_c [MPa]	Experimentation	42008	45405	43617	56309	54164
	Model	43003	43341	44255	52519	56845
	Rule of mixtures	53092	53815	55505	67571	72397
Discrepancy	Model	2.4%	4.6%	1.5%	6.7%	4.9%
	Rule of mixtures	26.4%	18.5%	27.3%	20%	33.7%

Thus,

$$\varepsilon_c = \sigma_m(1 - V_f)\left(\frac{1}{E_m} + \frac{1}{E_f}\langle\lambda(\bar{x})\rangle\eta_2^2\right). \tag{29}$$

The previous relations in eq 27 and 29 are derived with more details in previous publications [13,14].

The composite elastic modulus follows from the relation

$$E_c = \frac{\sigma_c}{\varepsilon_c},$$

$$E_c = \frac{1 + \langle\lambda(\bar{x})\rangle\eta_1^2\eta_2}{\frac{1}{E_m} + \frac{\langle\lambda(\bar{x})\rangle\eta_2^2}{E_f}} \tag{30}$$

where η_1 and η_2 are orientation factors. If $g(\phi, \psi)$ is the probabilistic density function for fiber orientation in the composite,

$$\eta_1 = \langle sin\ \phi\ cos\ \psi\rangle \int_0^{\pi/2}\int_0^{\pi/2} g(\phi, \psi) \times sin\ \phi\ cos\ \psi d\phi d\psi \tag{31}$$

$$\eta_2 = \langle sin^2\ \phi\ cos^2\ \psi\rangle \int_0^{\pi/2}\int_0^{\pi/2} g(\phi, \psi) \times sin^2\ \phi\ cos^2\ \psi d\phi d\psi. \tag{32}$$

Those integrals are in the sense of Stieltjes. For example, three-dimensional (3D) randomness: $g(\phi, \psi) = 2/\pi\ sin\ \phi$, $\eta_1 = 1/2$, $\eta_2 = 1/3$; two-dimensional (2D) randomness: $g(\phi, \psi) = 2/\pi$, $\eta_1 = 2/\pi$, $\eta_2 = 1/2$; Aligned fibers: $g(\phi, \psi)$ is a Dirac distribution; $\eta_1 = 1$; $\eta_2 = 1$.

In general, $g(\phi, \psi)$ can have any form. However, in calculating the orientation coefficients, one may consider the fact that for any fiber orientation, the fibers nearing the surface of a mold tend to be parallel to that surface. This effect depends strongly on the fabrication process and the composite dimensions. A very simple way to approximate this effect is illustrated in Figure 6, where a linear transition is suggested.

Parametric Study of the Model

The Effect of Matrix Porosity on the Composite Elastic Modulus

This effect is studied with the following parameters: $E_f = 10E_m = 200{,}000$ MPa, $a_f = 0.5$ mm^2, $l_f = 30$ mm, $c = 1.57$ mm, $V_f = 5\%$, $k = 1357$ N/mm^3, and $\xi_0 = 10\%$ (matrix initial porosity) (Figure 7). The increase of the

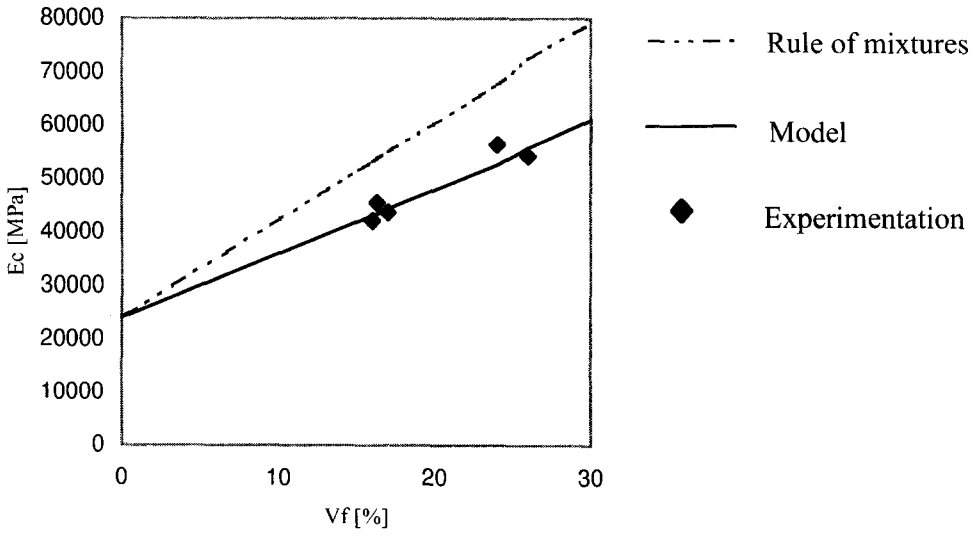

FIGURE 11. Illustration of the results from Table 2.

TABLE 3. Comparison between the test results and the model predictions

	V_f [%]	7	9.1	9.7	11.1	11.4
E_c [MPa]	Experimentation	15739	14989	16458	16398	17687
	Model 2D*	14832	16324	16769	17792	18038
	Model 3D*	14053	15296	15668	16525	16732
Discrepancy	Model 2D*	5.8%	8.9%	1.9%	8.5%	2.0%
	Model 3D*	10.7%	2.0%	4.8%	7.7%	5.4%

matrix porosity induces decrease in the composite elastic modulus.

Effect of the Bond Modulus K on the Elastic Modulus

Parameters of the study were: E_m = 20,000 MPa, $E_f = 2E_m$ (first case), $E_f = 0.5E_m$ (second case), a_f = 0.75 mm^2, l_f = 30 mm, c = 3.14 mm, ξ = constant, and aligned fibers (Figure 8). If $E_f \geq E_m$ the composite elastic modulus increases when the bond modulus increases. If $E_f \leq E_m$, the composite elastic modulus decreases when the bond modulus increases.

Experimental Validation of the Model

Uniaxial direct tension tests were conducted for cement composites with polypropylene, glass, and metallic fibers. The specimen geometry is given in Figure 9. The fabrication procedure was manual.

The test set-up is represented in Figure 10. A very low loading rate was used for the tests. The bond moduli were determined through direct pull-out tests on single fibers [13]. The evaluation of the bond modulus from the slope of the linear part of the pull-out curve was made with the help of the shear-lag concept [13].

Parameters for uniaxial tension tests (2D randomness assumed from specimen observation) were: polypropylene-FRC: E_f = 15,500 MPa, $E_m = E_{m0}$ = 19,000 MPa, a_f = 0.024 mm^2, l_f = 24 mm, c = 1.06 mm, and k = 378 N/mm^3; glass-FRC: E_f = 70,000 MPa, $E_m = E_{m0}$ = 70,000 MPa, a_f = 0.14 mm^2, l_f = 25 mm, c = 1.6 mm, and k = 1716 N/mm^3; metallic-FRC: E_f = 140,000 MPa, $E_m = E_{m0}$ = 140,000 MPa, a_f = 0.046 mm^2, l_f = 30 mm, c = 3.26 mm, and k = 1257 N/mm^3. Comparison of test results with model predictions is given in Table 1.

The elastic modulus was measured from the slope of the linear part of the direct tension test curve.

Tests from Literature (with High Fiber Volume Fraction)

STEEL-FRC IN UNIAXIAL TENSION. Tests performed by Alwan [15] included the following parameters: aligned fibers, E_f = 199,955 MPa, E_{m0} = 24,133 MPa, fiber diameter d_f

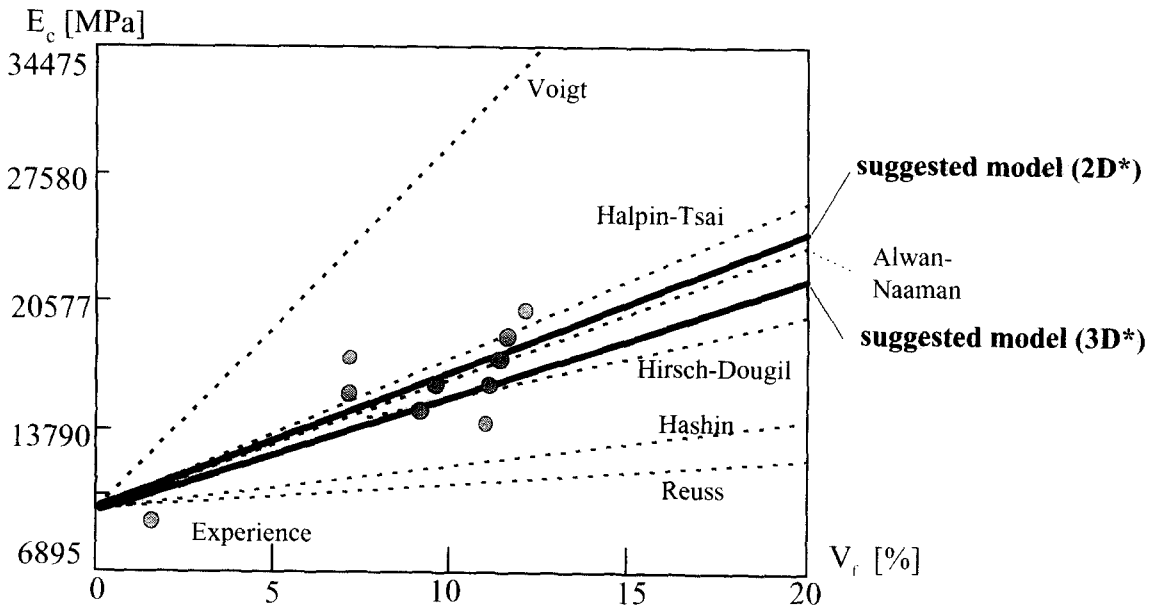

FIGURE 12. Graphical comparison between the test results, the model predictions, and the predictions of other models available in the literature. 2D* and 3D* = 2D and 3D randomness considering the effect due to the surface of the mold (see Figure 6).

= 0.48 mm, l_f = 30 mm, k = 1357 N/mm^3, and $\xi = \xi_0 + 0.25\ V_f = 0.08 + 0.25\ V_f$.

Comparison between the test results, the model predictions, and the rule of mixture predictions is displayed in Table 2 and illustrated in Figure 11.

STEEL-FRC IN UNIAXIAL TENSION. Tests from Alwan [15] and Lee et al. [16] included the following parameters: random oriented fibers, E_f = 199,955 MPa, E_{m0} = 24,133 MPa, fiber diameter d_f = 0.48 mm, l_f = 30 mm, k = 1357 N/mm^3, $\xi = \xi_0 + 0.25\ V_f = 0.08 + 0.25\ V_f$, and specimen cross section = 76/38 mm. Comparison between the test results and the model predictions is shown in Table 3. Graphical comparison of the experimental results with the model predictions and the predictions of other models available in the literature is shown in Figure 12.

Comment on the Results

For low fiber volume fraction (tests conducted by the authors), as one would expect, the discrepancy between the test results and the model predictions is very low. However, for high fiber volume fraction (tests from the literature), there is still good agreement between the experimental results and the model predictions. This can be explained by the fact that the bond modulus, the increase of the matrix porosity due to the presence of fibers, and the variation of the probabilistic density function of fiber orientation are taken into account in the model.

Conclusion

A new analytical model for predicting the elastic modulus for discontinuous fiber reinforced cement composites is presented. The model takes microstructural and probabilistic properties of the composite into account. The study shows that the interfacial bond modulus influences the global rigidity of the composite. Good agreement is observed between the model predictions and the limited experimental data available. The model can be used as a design tool to optimize the elastic properties of FRC and other fiber reinforced quasibrittle matrix composites. The model can also be used to determine the probabilistic parameters of fabrication processes.

References

1. Krenchel, H. *Fiber Reinforcement.* Akademisk Forlag, Copenhagen, 1988.
2. Nielsen, H.G.; Chen, E.L. *Journal of Materials* **1968,** *3(2),* 352–358.
3. Allen, H.G. *Composites* **1971,** *2,* 98–103.
4. Shah, S.P.; Rangan, B.V. *ACI Journal* **1971,** *68(2),* 126–135.
5. Pakoriprapha, B.; Pama, R.P.; Lee, S.L. *Magazine of Concrete Research* **1974,** *26(86),* 3–15.
6. Naaman, A.E.; Otter, D.; Najm, H. *ACI Material Journal* **1992,** *89(5),* 517–520.
7. Baalbaki, W.; Aitcin, P.C.; Ballivy, G. *ACI Material Journal* **1991,** *88(6),* 603–612.
8. Bentur, A. et al. In *High Performance Fiber Reinforced Cement Composite 2,* Naaman, A.E.; Reinhardt, H.W.; Spon, E.F.N. Eds.; **1995,** 149–191.
9. Alwan, J.M.; Naaman, A.E. New formulation for elastic modulus of fiber-reinforced quasibrittle matrices. *Journal of Engineering Mechanics* **1994,** *120(11),* 2443–2460.
10. Cox, H.L. *British Journal of Applied Physics* **1952,** *3,* 72–79.
11. Kendall, K. In *Physics and Chemistry in Porous Media,* Johnson, D.L.; Sen, P.N., Eds.; American Institute of Physics: New York, 1984.
12. Najm, H. Ph.D. Thesis, Department of Civil Engineering, University of Michigan, Ann Harbor, 1992.
13. Ngollè, A. Ph.D. Thesis, Institut National des Sciences Appliquées de Lyon, 1997.
14. Ngollè, A.; Pera, J. *Cement and Concrete Composites,* **1997,** submitted.
15. Alwan, J.M. Ph.D. Thesis, Department of Civil and Environmental Engineering, Univ. of Michigan, Ann Arbor, August 1994.
16. Li, V.C. et al. In *High Performance Fiber Reinforced Cement Composite 2;* Naaman, A.E.; Reinhardt, H.W.; Spon, E.P.N., Eds., **1995.**